Supporting Information

Supramolecular Functionalization for Improving Thermoelectric Properties of Single-Walled Carbon Nanotubes-Small Organic Molecule Hybrids

Jae Gyu Jang[a], Sun Young Woo[b], Hwankyu Lee[,b], Eunji Lee[*,c], Sung Hyun Kim[*,d] and Jong-In Hong[*,a]*

a. Department of Chemistry, Seoul National University, Seoul 08826, Korea.

b. Department of Chemical Engineering, Dankook University, Yongin 448-701, Korea.

c. School of Materials Science and Technology, Gwangju Institute of Science and Technology, Gwangju 61005, Korea.

d. Department of Carbon Convergence Engineering, Wonkwang University, Iksan 54538, Korea.

Corresponding Author

*E-mails: leeh@dankook.ac.kr (Hwankyu Lee), eunjilee@gist.ac.kr (Eunji Lee), shkim75@wku.ac.kr (Sung Hyun Kim), and jihong@snu.ac.kr (Jong-In Hong).

Syntheses of **1** and **2**

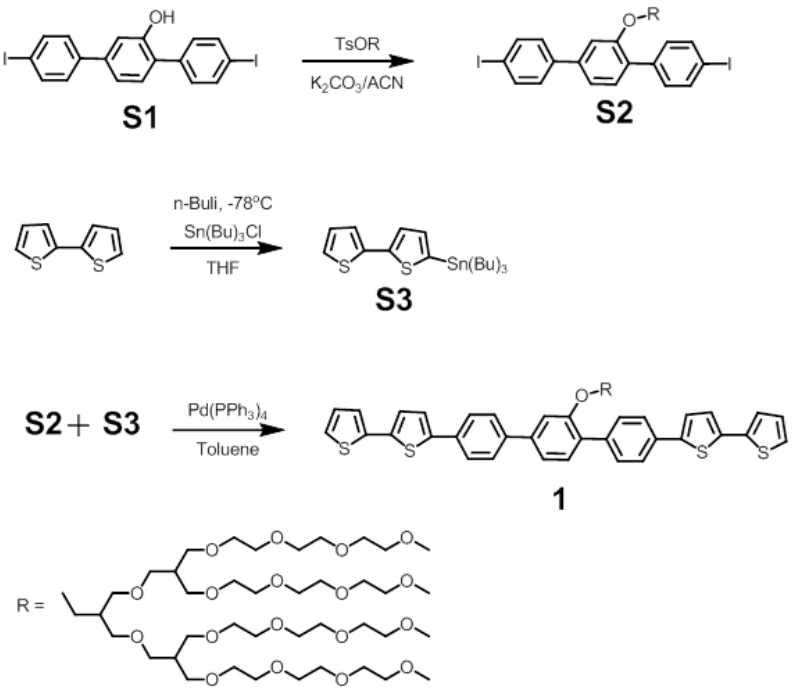

Scheme S1. Synthesis of amphiphile **1.**

Preparation for TsOR (Triethylene glycol monoether benzenesulfonate coils)

The second-generation dendritic triethylene glycol monoether benzenesulfonate coils were prepared as described previously.[1]

Synthesis of compound S1: S1 was prepared as described previously.[2] ^{1}H-NMR (300 MHz, $CDCl_3$) δ 7.83-7.76 (m, 4H), 7.41-7.32 (d, 5H), 7.24-7.22 (d, 1H, J = 6.1 Hz), 7.15 (s, 1H).

Synthesis of compound S2: S2 (200 mg, 0.40 mmol), R-OTs (341 mg, 0.33 mmol), and K_2CO_3 (555 mg, 4.02 mmol) were dissolved in 20 ml of acetonitrile. The mixture was heated at reflux for 48 h, and then cooled to room temperature. The resulting mixture was diluted with CH_2Cl_2. The organic phase was washed with water and dried over Na_2SO_4. The solvents were evaporated to afford a crude solid, which was purified by flash silica-gel column chromatography. Gradient elution from ethyl acetate to 10% methanol in ethyl acetate gave a

white solid (210 mg, yield: 40%). ^{1}H-NMR (300 MHz, $CDCl_3$) δ 7.80-7.73 (m, 4H), 7.44-7.24 (m, 5H), 7.21-7.16 (m, 2H), 4.11-4.09 (d, 2H, J = 4.9 Hz), 3.66-3.37 (m, 76H), 2.46 (s, 1H), 2.18-2.12 (m, 2H).

Synthesis of compound S3: n-Butyl lithium (n-BuLi, 1.6 M in hexane, 1.5 ml, 2.42 mmol) was added dropwise to a solution of 2,2′-bithiophene (280 mg, 1.68 mmol) dissolved in anhydrous tetrahydrofuran (20 mL) at −78 °C under N_2. The reaction mixture was stirred at −78 °C for 1 h. Tributyltin chloride (873 µl, 3.22 mmol) was added dropwise, stirred for 30 min at −78 °C, and then heated to room temperature. After 2 h, the crude product was diluted with CH_2Cl_2 and washed with water. The organic layer was dried over Na_2SO_4. The solvents were evaporated to afford a crude solid, which was chromatographed over triethylamine (TEA)-neutralized silica gel with hexane as an eluent, to give a light-yellow liquid (250 mg, yield: 33%). ^{1}H-NMR (300 MHz, $CDCl_3$) δ 7.39-7.38 (d, 1H, J = 3.2 Hz), 7.27-7.23 (d, 2H, J = 3.6 Hz), 7.17-7.15 (d, 1H, J = 3.3 Hz), 7.09-7.06 (dd, 1H, J = 3.7 Hz, J = 4.9 Hz) 1.74-1.64 (m, 6H), 1.52-1.40 (m, 6H), 1.25-1.14 (m, 6H), 1.04-0.99 (m,9H).

Synthesis of compound 1: A mixture of S2 (210 mg, 0.16 mmol), S3 (250 mg, 0.55 mmol), and tetrakis(triphenylphosphine) palladium (0) (18.5 mg, 0.016 mmol) was dissolved in dry toluene (20 ml) under a N_2 atmosphere. The mixture was refluxed for 24 h, and then cooled to room temperature. The resulting mixture was diluted with CH_2Cl_2 and washed with brine. The organic layer was dried over Na_2SO_4. Solvents were evaporated to afford a crude solid, which was purified by silica gel column chromatography with gradient elution from ethyl acetate to 10% methanol in ethyl acetate and further purified by recrystallization in hexane to yield a yellowish sticky solid (30 mg, yield: 13%). ^{1}H-NMR (300 MHz, $CDCl_3$) δ 7.71-7.58 (m, 8H), 7.47-7.44 (d, 1H, J = 7.8 Hz), 7.32-7.25 (m, 8H), 7.21-7.20 (d, 2H, J = 3.7 Hz), 7.08-7.05 (dd, 2H, J = 3.9 Hz, J = 4.8 Hz), 4.17-4.15 (d, 2H, J = 5.0 Hz), 3.64-3.37 (m, 76H), 2.40-2.36 (m, 1H), 2.19-2.17 (m, 2H). ^{13}C-NMR (75.47 MHz, $CDCl_3$) δ 156.39, 154.72, 143.00, 142.57,

141.16, 139.95, 137.38, 136.83, 133.29, 133.07, 132.55, 130.90, 130.10, 130.03, 127.90, 127.55, 125.97, 125.35, 125.29, 125.11, 125.03, 124.70, 124.45, 124.07, 123.86, 123.73, 123.68, 123.61, 119.44, 110.94, 71.92, 70.59, 70.55, 70.52, 70.50, 70.44, 69.66, 69.51, 69.26, 69.15, 59.00, 40.12. MALDI-TOF-MS m/z 1444.36 ($[M+Na]^+$), calcd 1444.57.

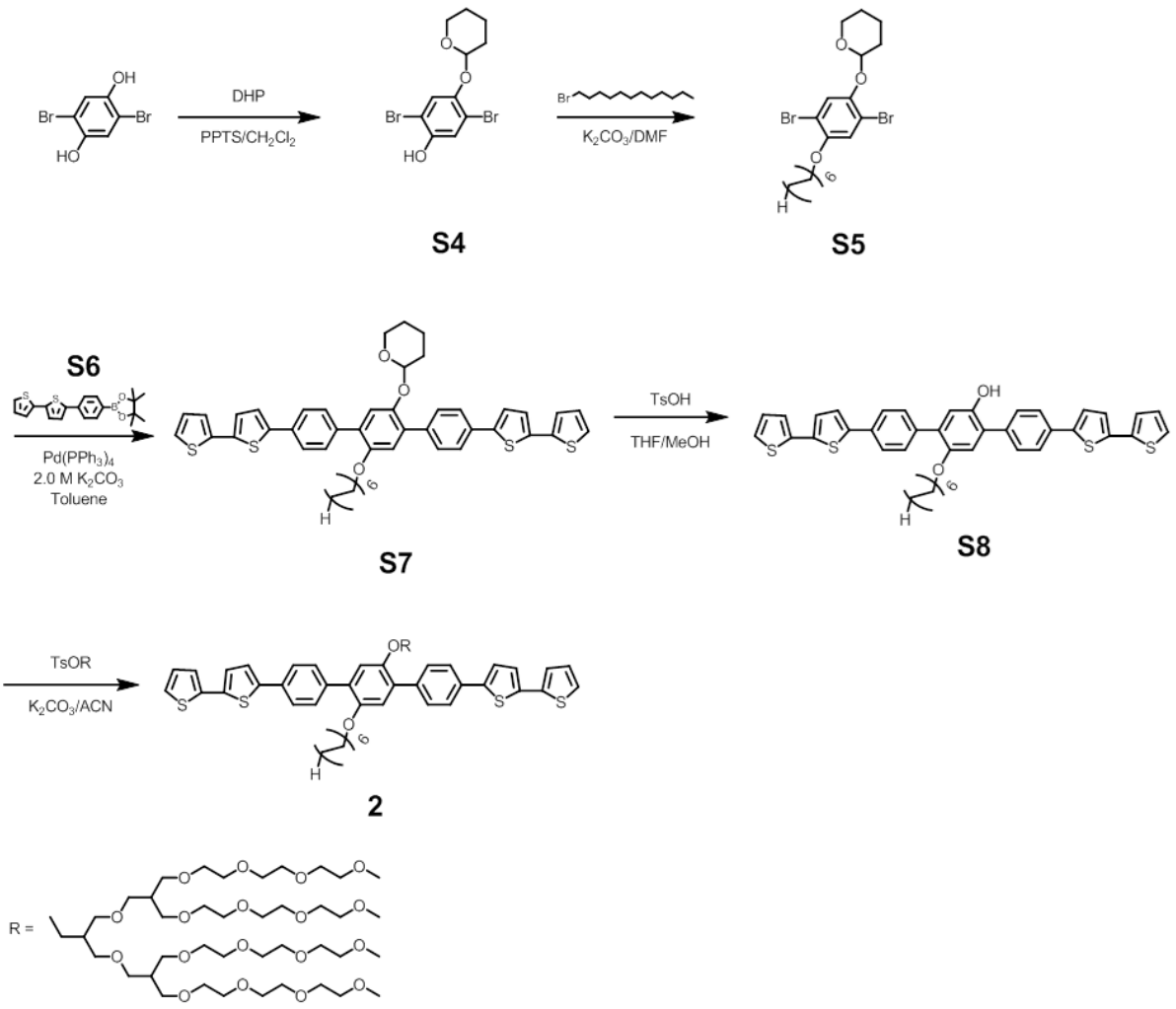

Scheme S2. Synthesis of amphiphile **2**.

Synthesis of compound S4: A mixture of pyridinium p-toluenesulfonate (PPTS, 5.0 mg, 0.02 mmol), 2,5-dibromohydroquinone (536 mg, 2 mmol), and 3,4-dihydro-2*H*-pyran (274 μl, 3.0 mmol) was dissolved in CH_2Cl_2 (20 ml). The reaction mixture was stirred overnight at room temperature. The mixture was diluted with CH_2Cl_2 and the combined organic layer was washed

with water and dried over Na_2SO_4. The solvents were removed under reduced pressure and the crude product was purified by silica gel column chromatography. Gradient elution from hexane to 10% ethyl acetate in hexane afforded a light-yellow liquid (320 mg, yield: 46 %). ^{1}H-NMR (300 MHz, $CDCl_3$) δ 7.28 (s, 1H), 7.20 (s, 1H), 5.35 (s, 1H), 3.97-3.90 (m, 1H), 3.67-3.63 (d, 1H, J = 10.89 Hz), 2.07-1.56 (m, 6H).

Synthesis of compound S5: A mixture of S4 (320 mg, 0.91 mmol), bromododecane (379 µl, 1.83 mmol), and K_2CO_3 (1.3 g, 9.14 mmol) was dissolved in 20 ml of DMF and heated at reflux overnight under a N_2 atmosphere. The reaction mixture was cooled to room temperature, diluted with water, and extracted twice with CH_2Cl_2. The combined organic layer was washed with water and dried over Na_2SO_4. The solvent was removed under reduced pressure and the crude material was purified by silica-gel column chromatography. Gradient elution from hexane to 10% ethyl acetate in hexane gave a light-yellow liquid (352 mg, yield: 75%). ^{1}H-NMR (300 MHz, $CDCl_3$) δ 7.38 (s, 1H), 7.07 (s, 1H), 5.36 (s, 1H), 3.98-3.88 (m, 3H), 3.65-3.61 (d, 1H, J = 10.82 Hz), 2.07-1.56 (m, 6H), 1.49-1.29 (m, 20H) 0.92-0.88 (m, 3H).

Synthesis of compound S6: S6 was prepared as described previously.[3] ^{1}H-NMR (300 MHz, $CDCl_3$) δ 7.85-7.82 (d, 2H, J = 8.06 Hz), 7.64-7.61 (d, 2H, J = 8.04 Hz), 7.32-7.23 (m, 3H), 7.17-7.15 (d, 1H, J = 5.88 Hz), 7.07-7.04 (dd, 1H, J = 3.74 Hz J = 4.84 Hz), 1.38 (s, 12H) [3].

Synthesis of compound S7: A mixture of S5 (352 mg, 0.68 mmol), S6 (750 mg, 2.04 mmol), K_2CO_3 (2.0 M in DI water, 5 mL), and tetrakis(triphenylphosphine) palladium(0) (79 mg, 0.068 mmol) in toluene (20 ml) was refluxed overnight under N_2. The reaction mixture was cooled to room temperature and diluted with CH_2Cl_2. The organic phase was washed with brine and dried over Na_2SO_4. The solvents were evaporated to yield a crude product, which was further recrystallized from 10% CH_2Cl_2 in methanol to give a yellow solid (227 mg, yield: 41%). ^{1}H-NMR (300 MHz, $CDCl_3$) δ 7.69-7.67 (d, 8H, J = 6.60 Hz), 7.33-7.19 (m, 9H), 7.08-7.05 (m,

2H), 7.03 (s, 1H), 5.34 (s, 1H), 4.01-3.99 (t, 2H, J = 6.64 Hz), 3.86-3.83 (t,1H J = 10.36 Hz), 3.60-3.56 (d, 1H, J = 11.36 Hz), 1.85-1.63 (m, 6H),1.41-1.27 (m, 20H), 0.91-0.86 (m, 3H).

Synthesis of compound S8: To a solution of S7 (227 mg, 0.28 mmol) in tetrahydrofuran/methanol (10:1 v/v, 20 ml) was added a catalytic amount of p-toluenesulfonic acid, and the resulting reaction mixture was stirred for 6 h at room temperature under N_2. The reaction mixture was diluted with water and extracted twice with CH_2Cl_2. The combined organic layer was washed with water and dried over Na_2SO_4. The solvents were removed under reduced pressure and the resulting residue was recrystallized from dichloromethane and methanol to produce a dark-yellow solid (yield: 129 mg, yield: 64%). ^{1}H-NMR (300 MHz, $CDCl_3$) δ 7.74-7.58 (m, 8H), 7.33-7.24 (m, 8H), 7.09-7.06 (m, 3H), 6.94 (s, 1H), 4.93 (s, 1H) 3.97-3.92 (t, 2H, J = 6.23 Hz), 1.40-1.26(m, 20H), 0.90-0.86 (m, 3H).

Synthesis of compound 2: The same procedure as that used for the preparation of compound S2 (129 mg, 0.18 mmol) was used. The residue was purified by silica-gel column chromatography with gradient elution from ethyl acetate to 10% methanol in ethyl acetate and recrystallized from hexane and dichloromethane (9:1) to give a yellowish sticky solid (yield: 103 mg, 36 %). ^{1}H-NMR (300 MHz, $CDCl_3$) δ 7.67-7.64 (m, 8H), 7.33-7.23 (m, 6H), 7.20-7.19 (m, 2H), 7.07-7.04 (m, 3H), 7.03 (s, 1H), 4.05-4.03 (d, 2H, J = 5.06 Hz), 3.96-3.92 (t, 2H, J = 6.22 Hz), 3.63-3.37 (m, 76H), 2.40-2.36 (m, 2H), 2.16-2.12 (m, 1H), 1.40-1.26(m, 20H), 0.90-0.86 (m, 3H). ^{13}C NMR (75.47 MHz, $CDCl_3$) 150.41, 150.32, 143.04, 142.95, 137.67, 137.63, 137.49, 137.45, 136.65, 132.68, 132.66, 130.35, 130.14, 130.09, 130.05, 127.90, 127.87, 125.12, 125.06, 124.7, 124.67, 124.40, 124.36, 123.77, 123.68, 123.63, 123.60, 116.08, 115.53, 71.93, 70.60, 70.56, 70.52, 70.50, 70.45, 69.78, 69.66, 69.48, 69.29, 67.50, 60.38, 40.13, 40.06, 31.92, 29.72, 29.37, 29.62, 29.39, 29.32, 26.13, 22.69. 21.03, 14.20, 14.12. MALDI-TOF-MS m/z 1628.74 ($[M+Na]^+$), calcd 1628.75.

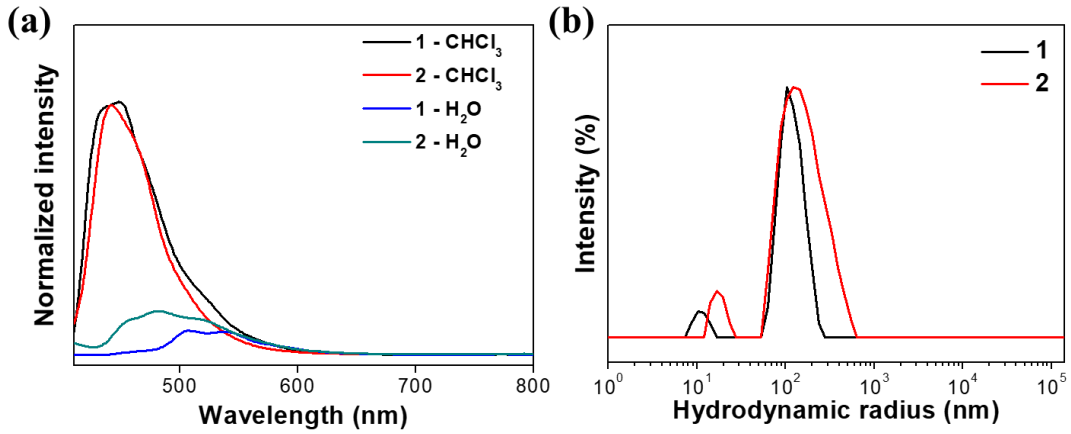

Figure S1. Emission spectra of (a) **1** and **2** (0.03 wt%, λ_{ex} = 386 nm) and (b) size distribution graphs of their aqueous solutions (0.03 wt%).

Solubility test of **1** and **2**

We evaluated solubilities of **1** and **2** in water as follows; (1) several different concentrations of **1** or **2** were made in water; (2) the aqueous solution of **1** or **2** was centrifuged at 13,000 rpm for 15 min. Then, we checked if the resultant solution was clear without any precipitates. The aqueous solution of **1** (0.06 wt%) and **2** (0.04 wt%) exhibited precipitates after centrifugation. However, the aqueous solutions of **1** (0.05 wt%) and **2** (0.03 wt%) were clear and free of any visible precipitates. Therefore, it turned out that the solubilities of **1** and **2** are < 0.06 wt% and < 0.04 wt%, respectively.

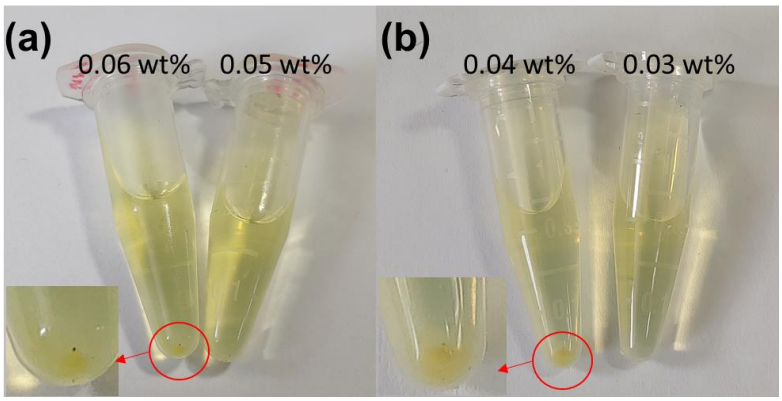

Figure S2. Photographs of (a) **1** (0.05 and 0.06 wt%) and (b) **2** (0.04 and 0.03 wt%) in an aqueous solution. Red circles and arrows indicate the precipitate of **1** (or **2**) after centrifugation at 13,000 rpm for 15 min.

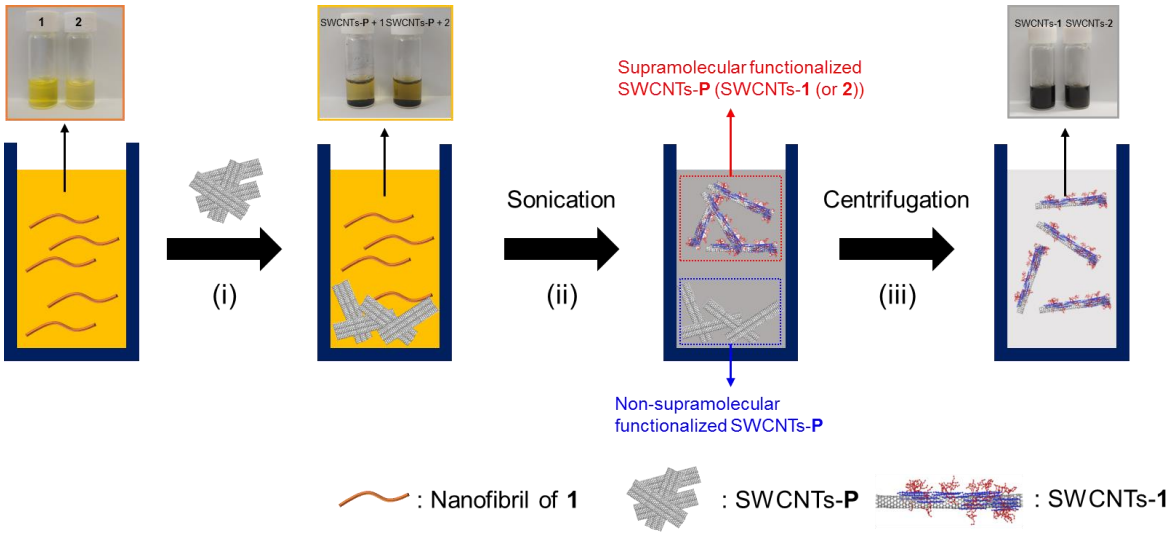

Figure S3. Schematic illustration for supramolecular functionalization of SWCNTs-**P** using **1** (or **2**): (i) Addition of SWCNTs-**P** (1 mg) to a 0.03 wt% aqueous solution of **1** (or **2**); (ii) bath-type sonication in a water-ice bath for 12 hours; (iii) centrifugation of the resultant solution at 13,000 rpm for 60 min. 70% of the supernatant was used for characterization and device studies. 0.03 wt% of **1** (or **2**) is an optimized concentration for supramolecular functionalization of SWCNTs-**P** because the liquid phase exfoliation of SWCNTs-**P** didn't occur at a 0.02 wt% **1** (or **2**) aqueous solution.[2-3]

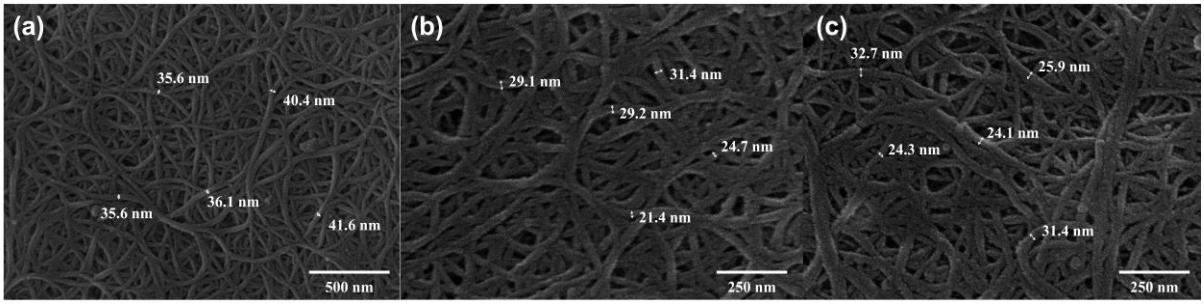

Figure S4. SEM image of (a) SWCNTs-**P**, (b) SWCNTs-**1**, and (c) SWCNTs-**2**. The average diameters of SWNCTs-**P**, SWCNTs-**1**, and SWCNTs-**2** are 37.9 nm with a standard deviation of 2.6 nm, 27.2 nm with a standard deviation of 3.6 nm, and 27.7 nm with a standard deviation of 3.6 nm.

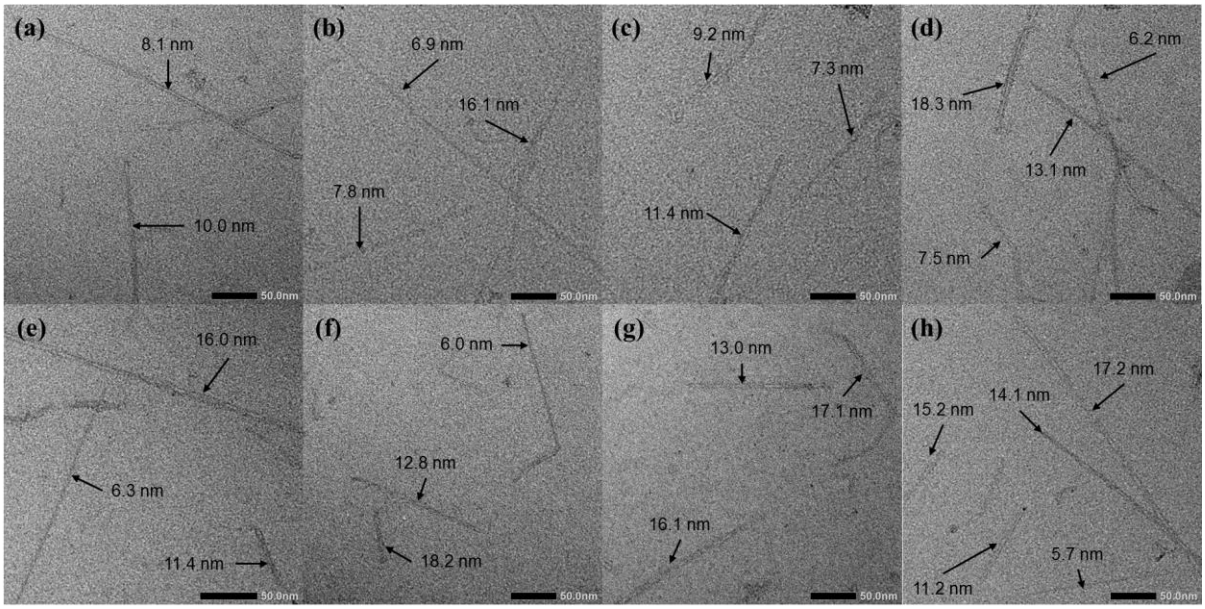

Figure S5. TEM images of (a)~(d) SWCNTs-**1** and (e)~(h) SWCNTs-**2**. The average diameters of SWCNTs-**1** and SWCNTs-**2** are 10.2 nm with a standard deviation of 3.7 nm and 12.9 nm with a standard deviation of 4.1 nm, respectively.

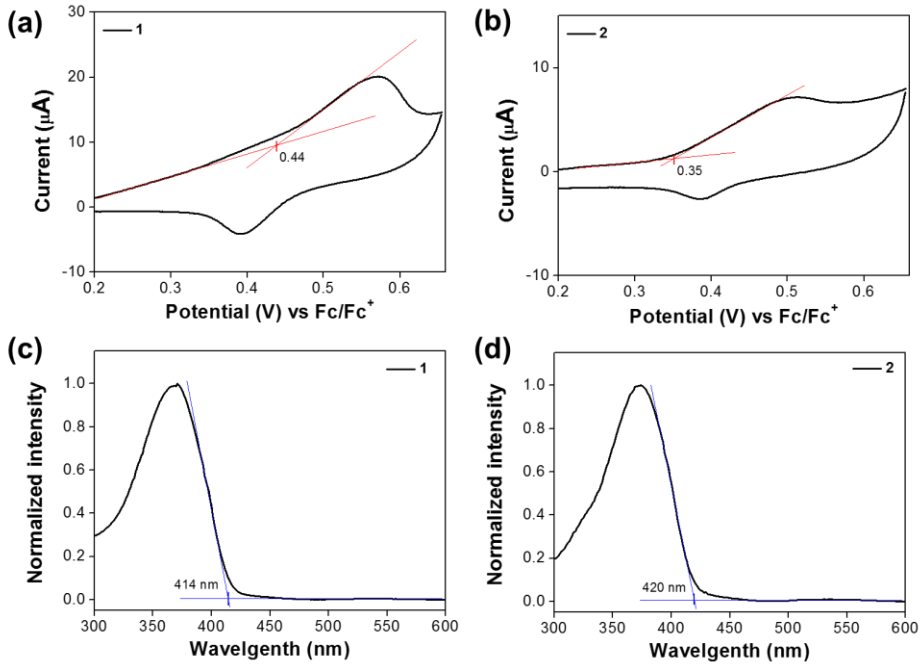

Figure S6. Cyclic voltammograms (CVs of (a) **1** (0.25 mM) and (b) **2 (**0.25 mM) with 0.1 M tetrabutylammonium perchlorate in methylene chloride. UV-Vis absorption spectra of (c) **1** (10 μM) and (d) **2** (10 μM) in methylene chloride. The red lines are onset potentials. Blue lines indicate optical band gaps; 2.99 and 2.95 eV for **1** and **2**, respectively.`

Charge-transfer interaction between SWCNTs-P and 1 (or 2)

Figure S7(a) shows the energy levels of SWCNTs-**P**, **1** and **2**. The slight red-shifts in absorption maxima of SWCNTs-**1** and SWCNTs-**2** were observed in Figure S7(b) and S7(c), indicating charge-transfer interactions. Although charge transfer from the valence band of SWCNTs-**P** to the LUMO of **1** (or **2**) showed large energy off-set, the G-band up shift and increased work function of SWCNTs-**1** (or **2**) strongly suggested that **1** (or **2**) acted as an electron acceptor.[4-11] Similar trend was also observed in previous reports (e.g. SWCNTs-**P**/oligo-phenylene vinylene derivatives[4], SWCNTs-**P**/poly(3-hexylthiophene) (P3HT)[5, 10], SWCNTs-**P**/dimethoxyphenylene-bisphenylthiophene derivatives[2], and MWCNTs-**P**/polyphenylene sulfide[6]). The charge transfer from SWCNTs-**P** to **1** (or **2**) can be attributed to thiophene moiety of **1** (or **2**). Lee group reported that sulfur of thiophene moiety extracted electrons from SWCNTs, showing G-band up-shift and increased work function of SWCNTs-**P**/P3HT composite.[10] SWCNTs-**P**/P3HT composite also exhibited G-band up-shift and increased work function.[5] Likewise, charge transfer occurred from SWCNTs-**P** to **1** (or **2**), which comes from charge-transfer interactions.

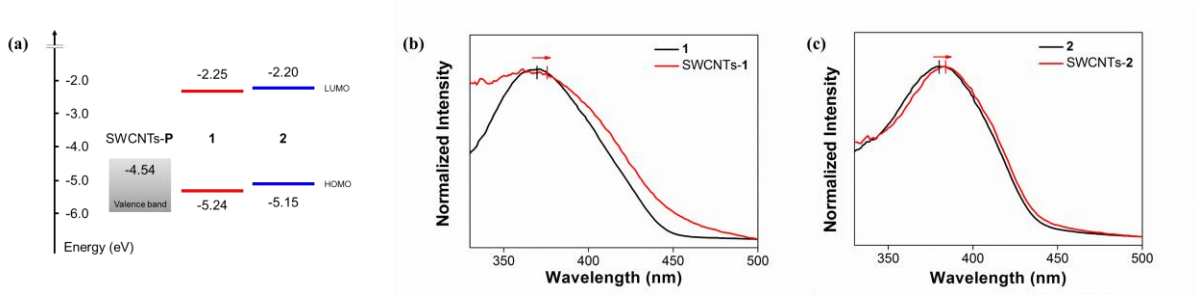

Figure S7. (a) Energy diagrams of SWCNTs-**P**, **1**, and **2**. HOMO and LUMO values of **1** and **2** were estimated from the onset potentials in CV experiments and optical band gap in UV-Vis absorption spectra, respectively. UV-Vis absorption spectra of (b) **1** (10 μM) and SWCNTs-**1** and (c) **2** (10 μM) and SWCNTs-**2** in aqueous solution.

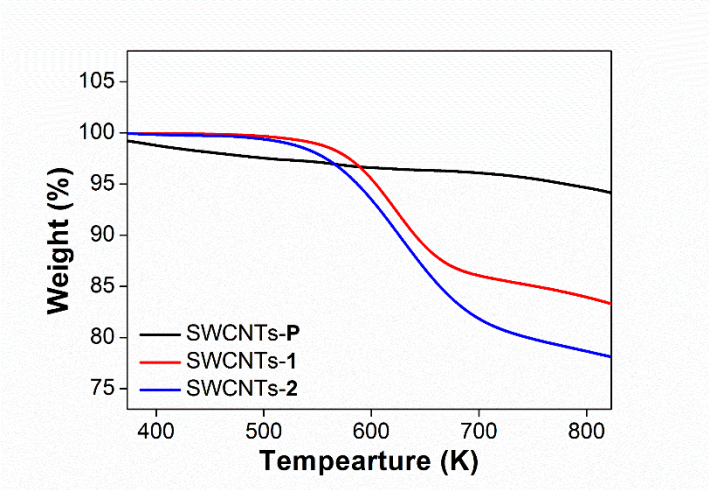

Figure S8. TGA curves of SWCNTs-**P**, SWCNTs-**1**, and SWCNTs-**2**.

UV-Vis absorption time-course experiments

The time-course adsorption ratio of amphiphiles (**1** or **2**) onto the SWCNT-**P** surface was estimated at their corresponding λ_{max} according to the Beer–Lambert law. During the sonication of the amphiphile-SWCNT-**P** mixture in aqueous solution at 273K, the samples were taken regularly and centrifuged for 30 min at 13,000 rpm to remove the nondispersed SWCNT-**P**. The supernatant was further centrifuged for 1 h at 18,000 rpm for removal of the SWCNT-**P**-amphiphile (**1** or **2**) complex. The solvent of the supernatant containing only free amphiphiles (**1** or **2**) was exchanged with chloroform to obtain clear monomeric absorption spectra. In addition, the adsorption ratio was estimated by the following equation:

$$\text{Adsorption ratio}(\%) = \frac{A_0 - A_t}{A_0} \times 100$$

Here, A_0 and A_t are the absorbance intensities of **1** or **2** at their corresponding λ_{max} before and after the dispersion process, respectively.

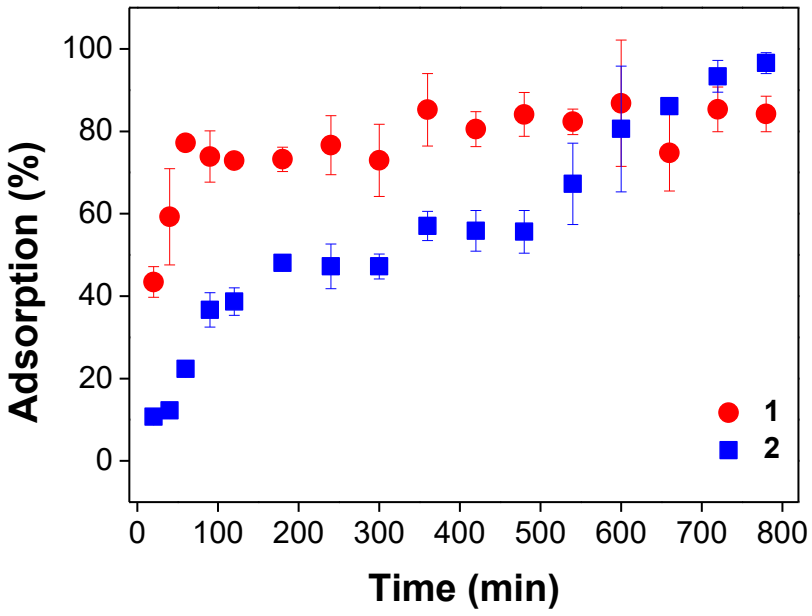

Figure S9. UV-Vis absorption time-course experiments of SWCNTs-**P** dispersion by **1** and **2**.

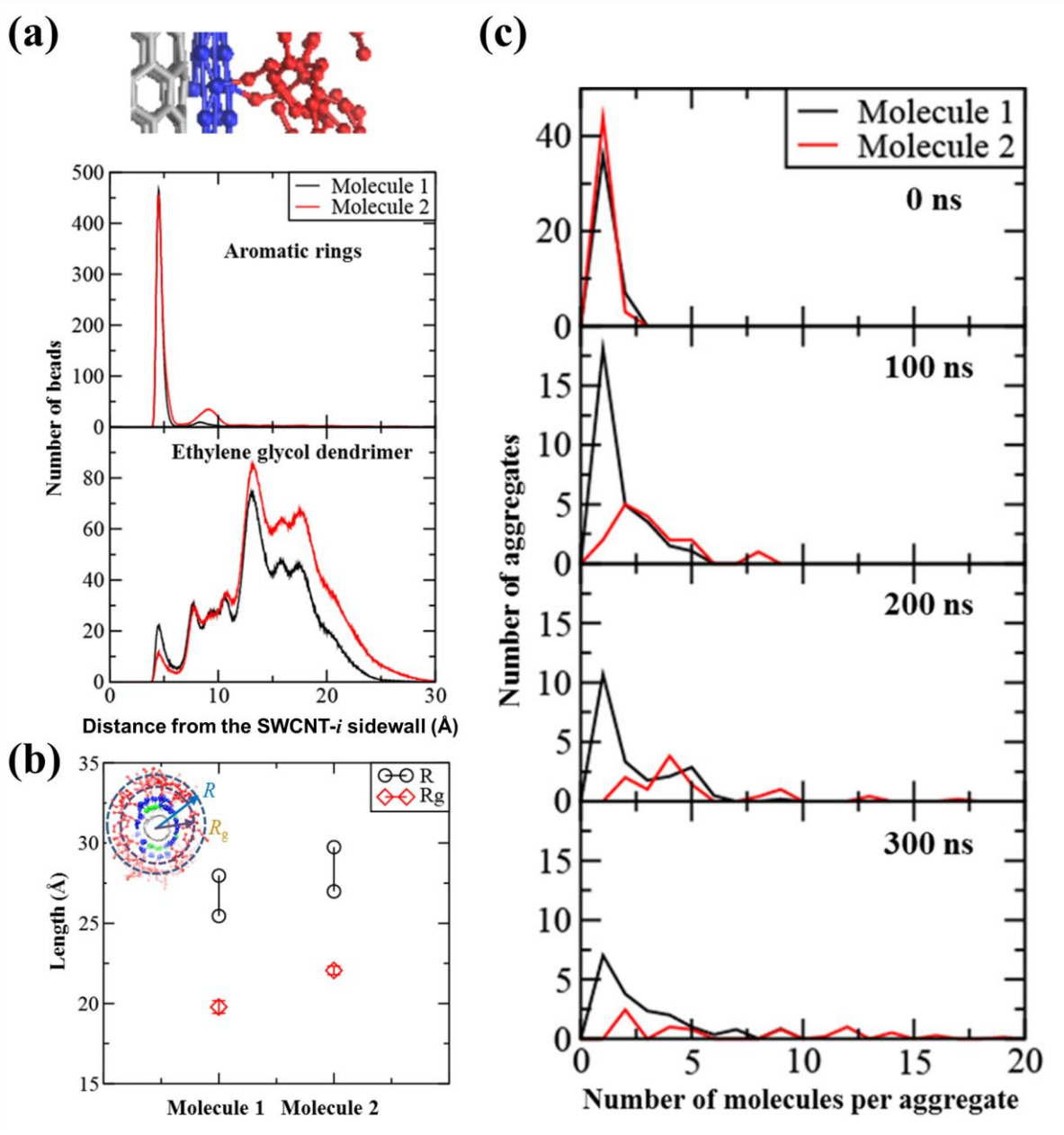

Figure S10. (a) Number of beads of aromatic rings and ethylene glycol dendrimers as a function of distance from the SWCNT-***i*** sidewall, (b) radii of gyration (R_g) and the outer radii (R) with respect to the end-on view of SWCNT-***i***. Here, R is defined as the distance between the COM of an SWCNT-***i*** and the height of PEG above the SWCNT-***i*** beads at which the PEG density falls to 85–95% of the maximum density, (c) distributions of the number of molecules per aggregate at 0, 100, 200, and 300 ns.

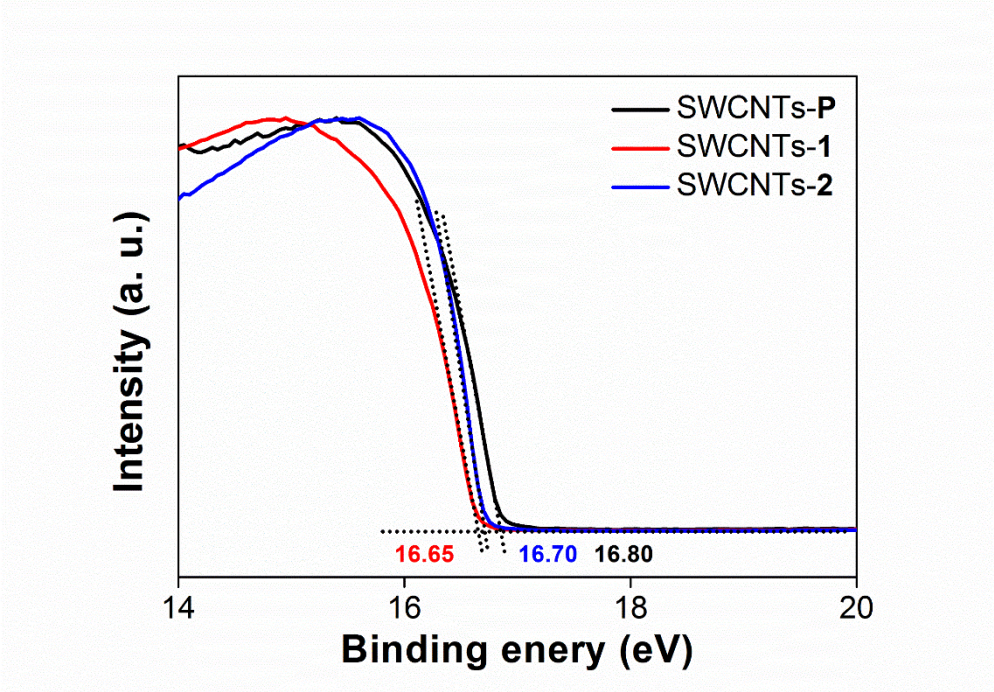

Figure S11. UV photoelectron spectroscopy spectra of SWCNTs-**P**, SWCNTs-**1**, and SWCNTs-**2** in the secondary-electron cutoff region.

π-π interaction between SWCNs-1 (or 2) and 1 (or 2)-mixed-SWCNTs

Figure S12 showed that the PL quenching of SWCNTs-**1** and SWCNTs-**2** were stronger than that of **1**-mixed-SWCNTs and **2**-mixed-SWCNTs. The G-bands of SWCNTs-**1** and SWCNTs-**2** exhibited up-shifted values. However, the G-bands of **1**-mixed-SWCNTs-**P**, and **2**-mixed-SWCNTs-**P** had similar values to that of SWCNTs-**P**. These results indicated that π-π interactions between **1** (or **2**) and SWCNTs-**P** in **1** (or **2**)-mixed-SWCNTs were weaker than SWCNTs-**1** (or **2**).[3, 12-13] In other words, electrostatic interactions between SWCNTs-**P** and **1** (or **2**) were poor in the **1** (or **2**)-mixed-SWCNTs, which didn't form charge-transfer interaction and enhance E_{Tr} - E_F.

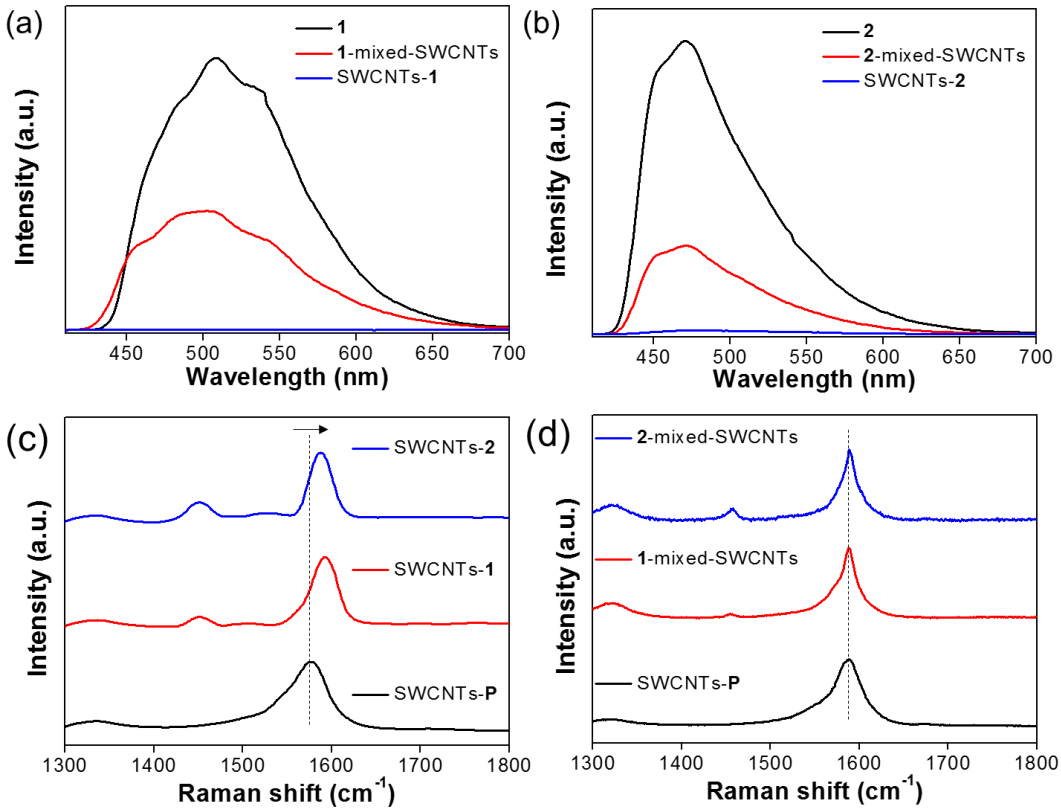

Figure S12. PL spectra of (a) **1**, **1**-mixed SWCNTs, and SWCNTs-**1** and (b) **2**, **2**-mixed-SWCNTs, and SWCNTs-**2** at λ_{ex} = 386 nm. Raman spectra of (c) SWCNTs-**P**, SWCNTs-**1**,

and SWCNTS-**2** obtained upon excitation at 532 nm excitation and (d) SWCNTs-**P**, **1**-mixed-SWCNTs-**P**, and **2**-mixed-SWCNTs-**P** obtained upon excitation at 633 nm.

Table S1. Thermal diffusivity, density, and specific heat capacity of SWCNTs-**P**, SWCNTs-**1**, and SWCNTs-**2**.

Sample	Thermal diffusivity [$\times 10^{-6}$, m^2/s]	Density [g/cm^3]	Specific heat capacity [J/gK]
SWCNTs-**P**	10.02	0.65	0.72
SWCNTs-**1**	8.78	0.47	0.80
SWCNTs-**2**	7.20	0.42	0.83

Table S2. Electrical conductivity and Seebeck coefficient of **1** (or **2**) physically mixed SWCNTs-**P** (without liquid-phase exfoliation).

Sample	Electrical conductivity [S/cm]	Seebeck coefficient [μV/K]
1-mixed-SWCNTs	25.71 ± 2.50	34.02 ± 5.95
2-mixed-SWCNTs	13.62 ± 1.21	34.30 ± 3.02

Table S3. Electrical conductivity and Seebeck coefficient of F_4TCNQ-doped SWCNTs-**1** and SWCNTs-**2** according to different doping time.

Doping time [min]	Electrical conductivity [S/cm]		Seebeck coefficient [μV/K]		Power Factor [μW/mK^2]	
	SWCNTs-**1**	SWCNTs-**2**	SWCNTs-**1**	SWCNTs-**2**	SWCNTs-**1**	SWCNTs-**2**
5	124.0 ± 5.2	279.3 ± 11.2	73.1 ± 4.2	65.0 ± 4.8	63.9 ± 10.1	128.9 ± 11.5
10	208.7 ± 11.0	338.7 ± 9.2	67.2 ± 3.1	62.5 ± 2.2	90.6 ± 11.5	144.5 ± 9.8
15	312.4 ± 9.9	542.9 ± 18.1	63.0 ± 4.4	56.7 ± 6.9	119.9 ± 9.8	190.5 ± 11.2
20	432.8 ± 21.2	629.3 ± 19.5	56.8 ± 5.7	50.8 ± 2.1	131.2 ±22.4	177.7 ± 14.5
30	755.5 ± 52.0	796.1 ± 63.1	29.0 ± 1.2	40.8 ± 3.2	61.4 ± 4.2	145.0 ± 13.1

Table S4. In-plane κ_{Total}, κ_L, and κ_E of F_4TCNQ-doped SWCNTs-**1** and SWCNTs-**2** at 300 K. The κ_{Total} values of F_4TCNQ-doped SWCNTs-**1** and SWCNTs-**2** were evaluated for the samples having maximum PFs.

Sample	κ_{Total} [W/mK]	κ_L [W/mK]	κ_E [W/mK]
F_4TCNQ-doped SWCNTs-**1**	3.36	3.04	0.32
F_4TCNQ-doped SWCNTs-**2**	2.91	2.51	0.40

REFERENCES

(1) Kim, H.-J.; Jung, E.-Y.; Jin, L. Y.; Lee, M. Solution behavior of dendrimer-coate d rodlike coordination polymers. *Macromolecules*, **2008**, *41*, 6066-6072.

(2) Lee, W.; Lee, D. W.; Lee, M.; Hong, J. I. Direct exfoliation of carbon allotropes with structural analogues of self-assembled nanostructures and their photovoltaic applic ations. *Chem. Commun.*, **2014**, *50*, 14851-14854.

(3) Lee, D.-W.; Kim, T.; Lee, M. An amphiphilic pyrene sheet for selective functiona lization of graphene. *Chem. Commun.*, **2011**, *47*, 8259-8261.

(4) Vedhanarayanan, B.; Nair, V. S.; Nair, V. C.; Ajayaghosh, A. Formation of Coaxi al Nanocables with Amplified Supramolecular Chirality through an Interaction between Carbon Nanotubes and a Chiral π-Gelator. *Angew. Chem. Int. Ed.*, **2016**, *128*, 10501-10505.

(5) Dabera, G. D. M.; Jayawardena, K. I.; Prabhath, M. R.; Yahya, I.; Tan, Y. Y.; N ismy, N. A.; Shiozawa, H.; Sauer, M.; Ruiz-Soria, G.; Ayala, P. Hybrid Carbon Nano tube Networks as Efficient Hole Extraction Layers for Organic Photovoltaics. *Acs Nan o*, **2013**, *7*, 556-565.

(6) Yang, J.; Xu, T.; Lu, A.; Zhang, Q.; Tan, H.; Fu, Q. Preparation and properties of poly (p-phenylene sulfide)/multiwall carbon nanotube composites obtained by melt c ompounding. *Compos. Sci. Technol.*, **2009**, *69*, 147-153.

(7) De Blauwe, K.; Kramberger, C.; Plank, W.; Kataura, H.; Pichler, T. Raman respo nse of FeCl3 intercalated single-wall carbon nanotubes at high doping. *Phys. Status S olidi B*, **2009**, *246*, 2732-2736.

(8) Zhang, S.; Park, J. G.; Nguyen, N.; Jolowsky, C.; Hao, A.; Liang, R. Ultra-high conductivity and metallic conduction mechanism of scale-up continuous carbon nanotu be sheets by mechanical stretching and stable chemical doping. *Carbon*, **2017**, *125*, 64

9-658.

(9) Shin, H. J.; Kim, S. M.; Yoon, S. M.; Benayad, A.; Kim, K. K.; Kim, S. J.; Par k, H. K.; Choi, J. Y.; Lee, Y. H. Tailoring Electronic Structures of Carbon Nanotube s by Solvent with Electron-Donating and -Withdrawing Groups. *J. Am. Chem. Soc.*, **2 008**, *130*, 2062-2066.

(10) Kim, K. K.; Yoon, S. M.; Choi, J. Y.; Lee, J.; Kim, B. K.; Kim, J. M.; Lee, J. H.; Paik, U.; Park, M. H.; Yang, C. W. Design of dispersants for the dispersion of carbon nanotubes in an organic solvent. *Adv. Funct. Mater.*, **2007**, *17*, 1775-1783.

(11) Rao, A. M.; Eklund, P.; Bandow, S.; Thess, A.; Smalley, R. E. Evidence for ch arge transfer in doped carbon nanotube bundles from Raman scattering. *Nature*, **1997**, *388*, 257-259.

(12) Jung, J.; Suh, E. H.; Jeong, Y. J.; Yang, H. S.; Lee, T.; Jang, J. Efficient Debu ndling of Few-Walled Carbon Nanotubes by Wrapping with Donor–Acceptor Polymers for Improving Thermoelectric Properties. *ACS Appl. Mater. Interfaces*, **2019**, *11*, 4733 0-47339.

(13) Goutam, P. J.; Singh, D. K.; Iyer, P. K. Photoluminescence quenching of poly (3-hexylthiophene) by carbon nanotubes. *J. Phys. Chem. C*, **2012**, *116*, 8196-8201.